

Elemental Analysis of *Mycobacterium avium*-, *Mycobacterium tuberculosis*-, and *Mycobacterium smegmatis*-Containing Phagosomes Indicates Pathogen-Induced Microenvironments within the Host Cell's Endosomal System¹

Dirk Wagner,^{2*†} Jörg Maser,^{2‡} Barry Lai,[‡] Zhonghou Cai,[‡] Clifton E. Barry III,[§] Kerstin Höner zu Bentrup,^{3¶} David G. Russell,[¶] and Luiz E. Bermudez^{4*}

Mycobacterium avium and *Mycobacterium tuberculosis* are human pathogens that infect and replicate within macrophages. Both organisms live in phagosomes that fail to fuse with lysosomes and have adapted their lifestyle to accommodate the changing environment within the endosomal system. Among the many environmental factors that could influence expression of bacterial genes are the concentrations of single elements within the phagosomes. We used a novel hard x-ray microprobe with suboptical spatial resolution to analyze characteristic x-ray fluorescence of 10 single elements inside phagosomes of macrophages infected with *M. tuberculosis* and *M. avium* or with avirulent *M. smegmatis*. The iron concentration decreased over time in phagosomes of macrophages infected with *Mycobacterium smegmatis* but increased in those infected with pathogenic mycobacteria. Autoradiography of infected macrophages incubated with ⁵⁹Fe-loaded transferrin demonstrated that the bacteria could acquire iron delivered via the endocytic route, confirming the results obtained in the x-ray microscopy. In addition, the concentrations of chlorine, calcium, potassium, manganese, copper, and zinc were shown to differ between the vacuole of pathogenic mycobacteria and *M. smegmatis*. Differences in the concentration of several elements between *M. avium* and *M. tuberculosis* vacuoles were also observed. Activation of macrophages with recombinant IFN- γ or TNF- α before infection altered the concentrations of elements in the phagosome, which was not observed in cells activated following infection. Siderophore knockout *M. tuberculosis* vacuoles exhibited retarded acquisition of iron compared with phagosomes with wild-type *M. tuberculosis*. This is a unique approach to define the environmental conditions within the pathogen-containing compartment. *The Journal of Immunology*, 2005, 174: 1491–1500.

Bacterial pathogens live in the challenging environments of the mammalian host by expressing virulence factors that enable them to survive and replicate. Environmental cues that have been found to modulate expression of bacterial genes include inorganic ion concentrations (1). Several virulence factors like Shiga toxin from *Shigella* or the diphtheria toxin from *Corynebacterium* are known to be regulated by the iron concentration (2, 3). The Yop system of *Yersinia*, which is associated with inhibition of phagocytosis, is regulated by low calcium concentration (4), and the PhoP/PhoQ two-component regulatory system of

Salmonella, which is necessary for intracellular survival, is regulated by the low magnesium concentration in the *Salmonella* phagosome (2, 5). Using reporter gene constructs, Garcia-del Portillo et al. (6) published data indicating that *Salmonella*-containing vacuoles in epithelial cells contain low concentrations of magnesium and iron. These observations suggest that some bacteria-containing vacuoles lack all or almost all necessary single elements, such as iron, and that this may represent a mechanism by which the host cell creates conditions adverse to foreign invaders. Despite the obvious importance of these elements to the infection process, no direct study of their concentrations has been undertaken.

Mycobacterium tuberculosis and *Mycobacterium avium* are important human pathogens responsible for the death of millions of individuals yearly (7, 8). Both *M. tuberculosis* and *M. avium* are intracellular pathogens that infect primarily mononuclear phagocytes. When inside macrophages and monocytes, *M. tuberculosis* and *M. avium* reside within cytoplasmic vacuoles that neither acidify nor fuse with lysosomes (9, 10). The phagosomal environment likely influences the expression of virulence genes of *M. tuberculosis* or *M. avium*.

It is well known that iron is a required element for growth and survival of *M. tuberculosis* in its host (11), and iron overload can be an exacerbating cofactor to tuberculosis (12, 13). Not only is iron important for growth but either iron or manganese is also part of the active center of stress-resistance proteins such as superoxide dismutase (SOD),⁵ a known scavenger of oxygen radicals. SOD

*Kuzell Institute for Arthritis and Infectious Diseases, San Francisco, CA 94115; [†]Department of Internal Medizin II Infectious Diseases, University of Freiburg, Freiburg, Germany; [‡]Experimental Facilities Division, Argonne National Laboratory, Argonne, IL 60439; [§]Tuberculosis Research Section, Laboratory of Host Defenses, National Institutes of Health, Rockville, MD 20852; and [¶]Department of Microbiology and Immunology, College of Veterinary Medicine, Cornell University, Ithaca, NY 14853

Received for publication August 18, 2003. Accepted for publication November 16, 2004.

The costs of publication of this article were defrayed in part by the payment of page charges. This article must therefore be hereby marked *advertisement* in accordance with 18 U.S.C. Section 1734 solely to indicate this fact.

¹ This work was supported by Grant ROI-AI 47010 of the National Institutes of Health and by the U.S. Department of Energy, Office of Basic Energy Sciences, under Contract W-31-109-Eng-38. D.W. was supported in part by a scholarship of the Walter-Marget-Wereinigung, Germany.

² D.W. and J.M. contributed equally to this study.

³ Current address: Tulane University, School of Medicine, Department of Microbiology and Immunology, New Orleans, LA 70112.

⁴ Address correspondence and reprint requests to Dr. Luiz E. Bermudez, Department of Biomedical Sciences, College of Veterinary Medicine, Oregon State University, 105 Magruder Hall, Corvallis, OR 97331. E-mail address: Luiz.Bermudez@oregonstate.edu

⁵ Abbreviations used in this paper: SOD, superoxide dismutase; NRAM, natural resistance-associated macrophage protein.

has been described in pathogenic *M. avium* and *M. tuberculosis* (14, 15). However, it is unclear whether the iron concentration in the mycobacterial phagosome in macrophages is limiting, as documented previously for *Salmonella*-containing vacuoles in epithelial cells. Researchers have tended to infer that the concentration of iron in phagosomes containing *Mycobacterium* spp. is limiting because of the extensive array of iron-binding moieties expressed by the bacterium (16, 17). However, the documented delivery of transferrin to *Mycobacterium*-containing vacuoles calls this interpretation into question (18–20).

To directly measure the concentration of the single elements such as iron within the mycobacterial phagosome, we used a novel technique, the hard x-ray microprobe with suboptical resolution. This system enables mapping of the trace element in a specimen by analyzing characteristic x-ray fluorescence spectra without the use of a fluorescence dye. Autoradiography of infected macrophages incubated with ^{59}Fe -loaded transferrin confirmed the measured increase of the iron concentration in the mycobacterial vacuole, supporting the hypothesis that the vacuolar iron is available to mycobacteria.

Materials and Methods

Mycobacteria

M. avium strain 101, a clinical isolate from the blood of an AIDS patient, has been previously described (21). *M. tuberculosis* H37Rv was purchased from American Type Culture Collection, *Mycobacterium smegmatis* mc²155 was kindly provided by W. Jacobs, Jr. (Albert Einstein School of Medicine, Bronx, NY), and the mutant H37Rv O1A was created as previously described (16). The bacteria were cultured as previously reported (16) on Middlebrook 7H11 agar.

Specimen preparation

Peritoneal macrophages from C57BL/6 (*bcg*^S) mice were isolated as described (21, 22) and grown for 18–24 h on sterile, formvar-coated London finder gold grids (Electron Microscopy Sciences) in RPMI 1640 supplemented with 10% FBS (Sigma-Aldrich). The monolayers were infected with *M. avium* (strain 101), *M. tuberculosis* (strain H37Rv), the siderophore knockout mutant of *M. tuberculosis* strain H37Rv (*Mtb* H37Rv O1A) or *M. smegmatis* (strain mc² 155) for 1 h with an approximate ratio of 10 bacteria per macrophage. The viability of the inoculum was determined by using the LIVE-DEAD (Molecular Probes) assay as previously reported (21). Only inocula with at least 90% viability were used for the assays. After 1 and 24 h of infection, the macrophages were washed twice with HBSS to remove the remaining extracellular bacteria and fixed in 1% paraformaldehyde (pH 7.2) for 30 min. The electron microscopy grids were then washed in HBSS twice, rinsed shortly with sterile water, air-dried, and then kept at room temperature in viewing chambers for the microscopic identification of bacteria or phagosomes. Recombinant murine IFN- γ and recombinant murine TNF- α (purchased from BioSource) were used to stimulate the macrophages. Treatment of peritoneal macrophages with 10^2 U/ml IFN- γ or 10^2 U/ml TNF- α were performed 24 h before or 24 h after infection with *M. avium*. Macrophage monolayers remained exposed to cytokines for 24 h. Extracellular bacteria that were not removed by the washing were fixed after 1 h of infection and used as a source of extracellular bacteria for the measures.

Hard x-ray microprobe

This technique directly (physically) measures the elemental concentrations, combining high elemental sensitivity (subfemtogram) and low background with suboptical spatial resolution (150 nm). The hard x-ray microprobe (23) that was used to collect maps of the elemental distribution in the macrophage and the phagosome operates at the Advanced Photon Source, a third generation synchrotron that produces tunable hard x-rays with high intensity and collimation in a small spectra band. Direct excitation of atomic K or L transitions of all elements in the periodic system is possible by tuning the incident x-ray energy to a value between 6 and 30 keV. We chose an incident energy of 10 keV, which allowed efficient excitation of elements with a Z number up to 30 (Zn) at highest spatial resolution. Due to absence of bremsstrahlung from inelastically scattered charged particles, as is encountered in electron or proton microprobes, the background in the x-ray microprobe is significantly smaller, yielding an intrinsic sensitivity of better than micromolar. Use of monochromatic x-rays for excitation con-

finer background from elastic and inelastic photon scattering to the high-energy side of the detected x-ray spectra, where it can easily be separated from the fluorescence signal that is unique to individual elements. Biological specimens as thick as 50–100 μm can be penetrated at sub-200-nm resolution, without any widening of the probing beam, as is encountered in electron microprobes. Therefore, no physical sectioning of the specimen is needed. In fact, whole macrophages are examined here without any sectioning. To map the elemental distribution, the specimen is placed on a motorized scanning stage, and raster scanned through the x-ray spot. An energy-dispersive ultra-LEGe detector (Canberra) with a spectral resolution of 180 eV is used to record the fluorescence spectra at each specimen point. A schematic representation of the hard x-ray beamline with the microprobe is shown in Fig. 1. Depending on the concentration of the element in question and specimen-intrinsic background, dwell times of 1–20 s are required for each pixel. In the simplest data analysis mode, spectra obtained at each pixel are filtered around the energies of K_{α} radiation of the elements of interest, allowing simultaneous mapping of currently up to 10 elements. The resulting elemental composition is mapped against the *x* and *y* position to yield an elemental map of the specimen. By normalizing the measured signal with data obtained from a calibration standard, fully quantitative maps of the elemental distribution are obtained for potassium, calcium, manganese, iron, copper, and zinc. For elements such as phosphorus, sulfur, chlorine, and nickel, where no calibration standards are available at the moment, relative concentrations are used.

Position of the x-ray probe on the phagosome

The macrophage and the region containing the phagosome were preselected using the optical microscope and specific coordinates were assigned to the vacuole using finder grids and the same kinematic mounts in the optical microscope and in the microprobe. A coarse scan on the macrophage, taken with a pixel size of $1 \times 1 \mu\text{m}$ at large photon flux ($\sim 2 \times 10^9$ photons/s) allowed the superimposition of the microscopic image with the scan and, together with the assigned coordinates, clear identification of the region containing the phagosomes. Then, a high resolution scan of the phagosome, with a pixel size of usually $0.2 \times 0.2 \mu\text{m}$ and correspondingly reduced photon flux ($\sim 2 \times 10^8$ photons/s) was taken, yielding 10 elemental maps.

Data analysis

Independent of the mycobacterial species, comparison of the microscopic image and the scans showed that the bacterial shape was outlined by the chlorine or the potassium distribution. These elements were therefore used as one of the parameters to precisely define the phagosomal/bacterial region of interest. In the same scan, a background region was defined next to the respective phagosome, omitting structures of the macrophage either visible in the light microscopic image or detected in the different images of the scan that could have adversely influenced the background counts. The mean count rate of this background was subtracted from the mean count rate of the phagosomal/bacterial region to yield the mean phagosome/bacteria count rate. The mean counts were normalized with synchrotron current and exposure time. For quantitation of elemental concentrations, thin-film standards with a known concentration of the respective element were available (National Institute of Standards and Technology/National Bureau of Standards (NBS) 1832, NBS 1833) were used. The yield of absolute atomic concentration in area density (nanograms per square centimeter) for elements (potassium, calcium, iron, copper, manganese, and zinc) using the molar mass of the respective elements and assuming the median thickness of mycobacteria to be $1 \mu\text{m}$, these data can be expressed as millimoles per liter or micromoles per liter. For elements where no standard was available (phosphorus, sulfur, chlorine, and nickel), the normalized signal in counts per second per A was used for further analysis. As a control, we used latex beads. Macrophages were allowed to take up latex beads, and macrophage monolayers were fixed and prepared 1 and 24 h after uptake, as described above. The concentration of elements on the beads was measured and calculated as follows: region of interest (ROI) for the latex beads was defined with identical geometry. One ROI, with diameter of $1 \mu\text{m}$, was placed in the center. ROI2 was centered around the latex bead. A thickness of 200 nm was taken into consideration. Statistical analysis was performed using Student's *t* test in the InStat computer program. A value of $p < 0.05$ was considered significant. The number (*n*) of mapped phagosomes per group is indicated in the tables.

Incubation with iron transferrin

Mouse bone marrow-derived macrophage monolayers were infected with *M. avium* 101, and the infection was left to establish for 4 days. The cultures were incubated overnight in medium with transferrin-depleted serum before experimentation. Human transferrin was stripped of iron and reloaded with ^{59}Fe (Amersham Biosciences) as described previously by

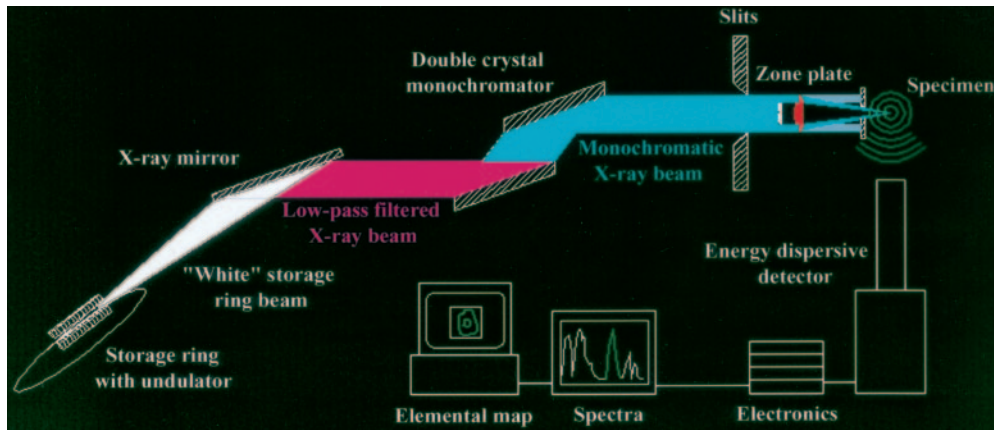


FIGURE 1. The hard x-ray microprobe in operation at the Advanced Photon Source. X-rays from the storage ring are low-pass filtered by an x-ray mirror, and monochromatized to a spectral bandwidth of $\Delta\lambda/\lambda = 10^{-4}$ by perfect silicon crystals. The monochromatic x-ray beam is focused on the sample by a Fresnel zone plate, yielding a monochromatic photon flux of 2×10^8 photons/s in a spot with 150-nm diameter. Apertures are used to reject unwanted background radiation and diffraction orders. The focused x-ray beam creates excited states of a fraction of the atoms in the sampled volume that decay by emitting secondary signals, such as x-ray fluorescence photons and Auger electrons. By analyzing the energy spectra of the emitted fluorescence photons, the elemental composition of the illuminated specimen volume can be directly measured.

Dyer et al. (24) and separated from free ^{59}Fe by two sequential passages over 10-ml gel filtration columns (Pierce). Labeled transferrin (10 $\mu\text{g}/\text{ml}$) was added to the infected macrophage cultures in the presence or absence of 100 $\mu\text{g}/\text{ml}$ unlabeled transferrin. The cultures were incubated overnight with the added transferrin and either fixed and processed for electron microscopy or rinsed and chased for 2 days before fixation and processing. The cultures were fixed in 1% glutaraldehyde in PBS, postfixed OsO_4 , and dehydrated through an ethanol series before embedding in Spurr's resin.

Sections were cut and stained with uranyl acetate and Reynold's lead boro coating with autoradiography emulsion EM1 (Amersham Biosciences), as detailed previously (25). The samples were incubated in the presence of a 10-fold excess of unlabeled transferrin and showed signal levels $<5\%$ of the experimental samples.

The relative distribution of specific signal was calculated from 20 negatives taken at $\times 6000$ magnification from each condition and time point. The number of decay traces associated with the cell cytoplasm, bacteria,

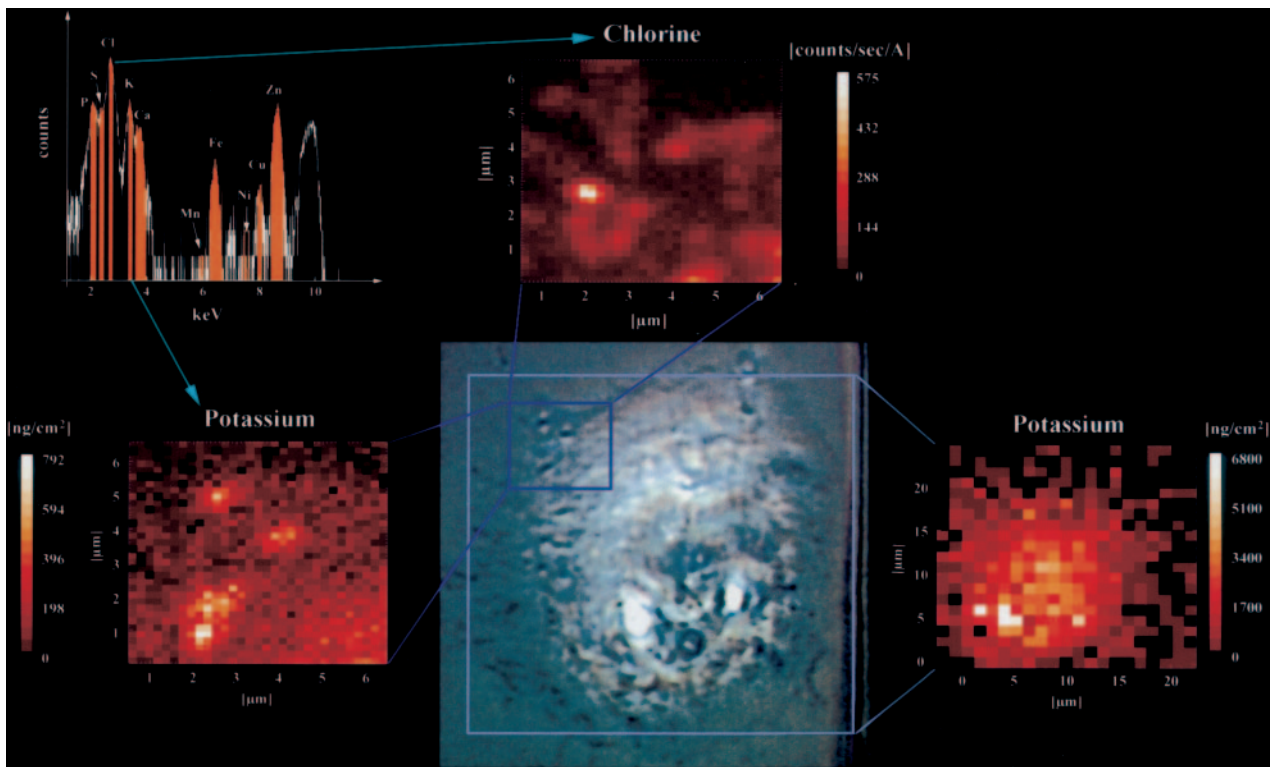


FIGURE 2. Allocation of the phagosome and data analysis. The incident x-ray beam excites the elements in the illuminated specimen volume for a preset time. Fluorescence photons emitted into the sensitive volume of the energy dispersive detector are pulse-height discriminated, and the resulting spectra filtered for fluorescence energies corresponding to up to 10 elements of interest (top left). A coarse scan on the macrophage (left), taken with a pixel size of $1 \times 1 \mu\text{m}$ at large photon flux (around 2×10^9 photons/s) allowed the superimposition of the microscopic image (center) with the scan and, together with the assigned coordinates, clear identification of the region containing the phagosomes (small box). Then, a high resolution scan of the phagosome, with a pixel size of usually $0.2 \times 0.2 \mu\text{m}$ and correspondingly reduced photon flux (around 2×10^8 photons/s) was taken, yielding 10 elemental maps. Elemental maps for potassium (right center) and chlorine (top center) are shown.

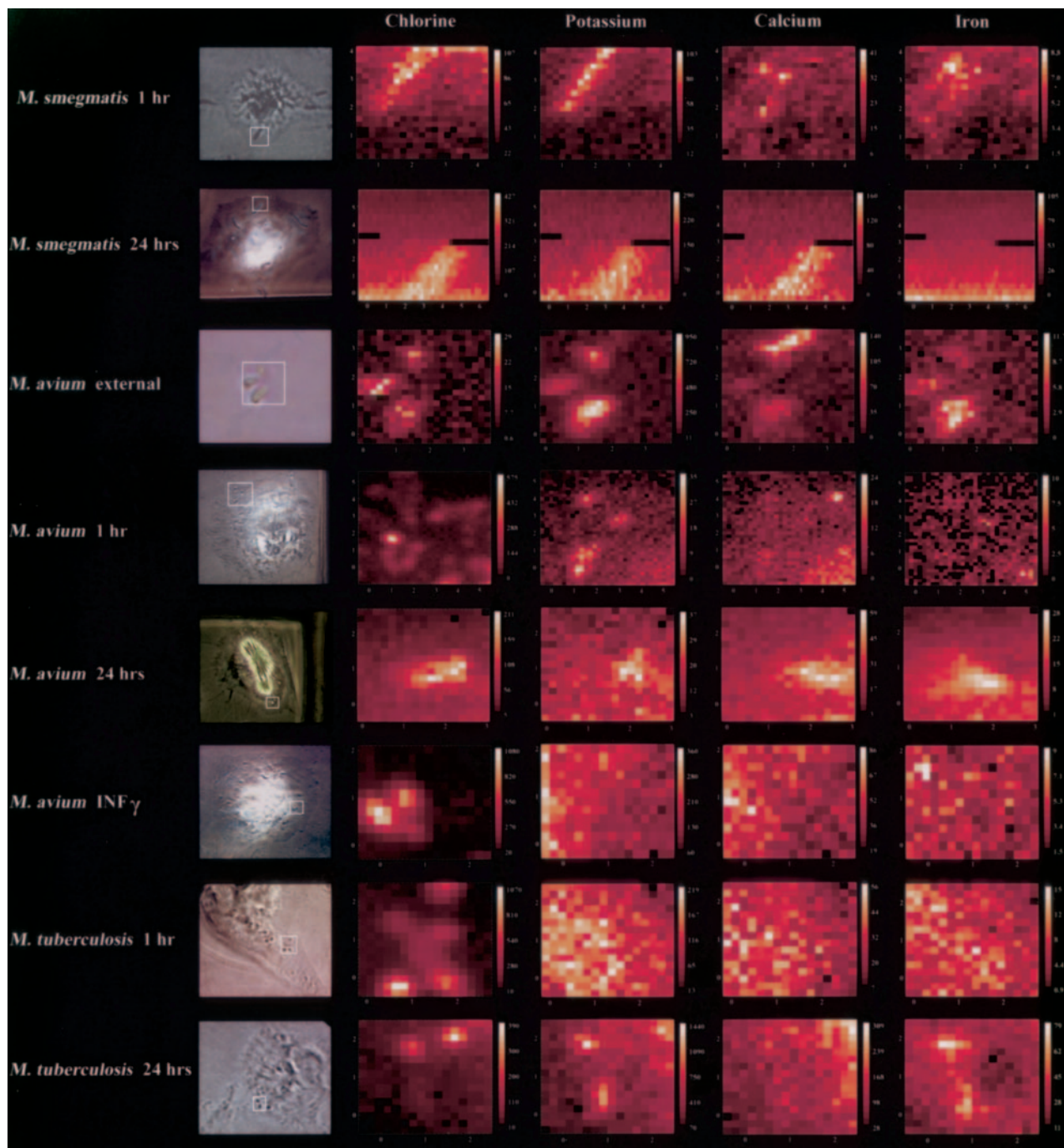


FIGURE 3. Elemental maps for chlorine, potassium, calcium, and iron for selected phagosomes. Examples of macrophages infected for 1 or 24 h with *M. smegmatis* (rows 1 and 2), *M. avium* (rows 4 and 5), or *M. tuberculosis* (rows 7 and 8), as well as external bacteria (an example of external *M. avium* is shown in row 3), and IFN- γ pretreated macrophages infected with *M. avium* for 24 h (row 6) are shown. Macrophages with intracellular mycobacteria were identified by light microscopy (left column), and the elemental distribution of the selected phagosome was mapped at a pixel size of $0.2 \times 0.2 \mu\text{m}$. The scanned region is represented by the white box in each respective light microscopical image. The elemental maps of chlorine, potassium, calcium, and iron (columns 2, 3, 4, and 5, respectively) for the respective macrophage are shown as examples. The scale on the x- and y-axes denotes the size in micrometers; the scale bar on the side of each elemental map expresses the concentration of the respective element in counts per second per A for chlorine and nanograms per square centimeter for potassium, calcium, and iron.

and nuclei were scored, corrected for relative surface area, and displayed as a histogram showing signal density per square micrometer.

Results

Intravacuolar concentration of single elements

We used a hard x-ray microprobe beamline (Fig. 1) to perform a quantitative analysis of the intravacuolar concentrations of 10 single

elements. The respective experiments were conducted during several runs during a period of 2 years. Before, during, and after each experiment, the instrument was calibrated using the thin-film standards. The variability of quantification within a run and between different runs was 5–10%. Measurements were conducted in macrophages infected with *M. avium*, *M. tuberculosis*, or *M. smegmatis* at 1 and 24 h following infection. Fig. 2 shows the allocation of the

phagosomes; Fig. 3 shows representative elemental maps for four different elements and the respective microscopic image of the mapped phagosome.

The values obtained are discussed as concentrations in the vacuoles, because the current resolution level does not allow discrimination between the vacuole and the bacteria within the vacuole (Table I). It was observed that the concentrations of phosphorus and sulfur did not change significantly over time inside of *M. avium*, *M. tuberculosis*, and *M. smegmatis* vacuoles but were significantly different at 1 h of infection when *M. smegmatis* vacuoles were compared. Similarly, the nickel concentration did not change over the time course of the infection in the different species, but was significantly higher at 1 h of infection in the *M. avium* vacuole compared with the *M. tuberculosis* vacuole. The zinc concentration was lower in the *M. tuberculosis* vacuoles at 1 h of infection than in the *M. avium* vacuole but increased after 24 h of infection.

In contrast, the concentration of chlorine increased in the *M. tuberculosis* vacuole during the first hour of infection, being significantly higher compared with the *M. smegmatis* and *M. avium* vacuoles, and decreased to a concentration closer to the concentration found in *M. avium* vacuole at 24 h.

The manganese concentration decreased in *M. smegmatis* vacuoles from 1 to 24 h after uptake by macrophages and was signif-

icantly lower at the later time point when compared with *M. avium* vacuoles. Changes that were observed in potassium, calcium, and copper concentrations did not reach statistical significance.

As control, macrophages were infected with latex beads, and the concentration of single elements was determined. Table II shows that latex beads do not appear to contain any metal.

Concentration of iron and elemental concentration in the siderophore knockout mutant

Given the known role of iron in bacterial growth and intracellular survival, we paid particular attention to its concentration within the vacuole. We observed that the concentration of iron in *M. smegmatis* phagosomes 1 h after bacterial uptake by macrophages was significantly higher in *M. avium* or *M. tuberculosis* phagosomes but decreased significantly with time. In contrast, the concentration of iron in both *M. avium* and *M. tuberculosis* vacuoles increased significantly between 1 and 24 h following uptake (Table III).

Iron acquisition by *M. tuberculosis* is achieved through the activity of siderophores and mycobactins. To determine whether these molecules play an active role in iron sequestration inside the macrophage, we infected macrophages with the strain H37Rv 01A, in which the gene encoding for the bacterial siderophore was inactivated (16). In vacuoles of this mutant, we saw an increased iron

Table I. Average concentration of trace elements in the mycobacterial phagosome^a

Unit	Element	Treatment	Mycobacterial Species		
			<i>M. smegmatis</i>	<i>M. avium</i>	<i>M. tuberculosis</i>
counts/s/A	Phosphorus	extern	20.4 ± 0.03 ^b	9.2 ± 1.2	6.5 ± 3.1
		1 h	22.7 ± 8.5	14 ± 6.5	7.0 ± 1.7 ^c
		24 h	9.5 ± 2.3	10.9 ± 2.1	7.1 ± 1.4
	Sulfur	extern	5.0 ± 1.4	2.7 ± 0.4	5.7 ± 2.4
		1 h	17.6 ± 5.3	18.5 ± 6.9	36.9 ± 5.5 ^c
		24 h	12.9 ± 9.2	35.9 ± 9.5	23.7 ± 3.9
	Chlorine	extern	33.4 ± 2.6	28.2 ± 13.4	42.6 ± 27.0
		1 h	61.7 ± 12.7	152 ± 106	404 ± 56 ^{c,d}
		24 h	107 ± 57.7	245 ± 150	197 ± 62
	Nickel	extern	0	2.3 ± 2.2	0.58 ± 0.58
		1 h	0.31 ± 0.31	0.97 ± 0.7 ^c	0.15 ± 0.06
		24 h	0.24 ± 0.13	1.0 ± 0.3	0.07 ± 0.05
mmol/L	Potassium	extern	30.2 ± 9	51.7 ± 15.4	40.7 ± 13.2
		1 h	20.3 ± 5.5	36.8 ± 15.7	19.5 ± 16.9
		24 h	14.1 ± 6.1	5.5 ± 2.9	51.0 ± 28.6
	Calcium	extern	2.3 ± 0.6	5.9 ± 2.5	16.3 ± 14.6
		1 h	2.0 ± 0.1	4.1 ± 1.5	1.8 ± 1.3
		24 h	4.6 ± 2.3	2.5 ± 1.1	7.1 ± 3.3
	Manganese	extern	7.5 ± 2.8	60.2 ± 32	15.8 ± 15.8
		1 h	18.9 ± 1.3	11.8 ± 4.4	14.7 ± 5.2
		24 h	4.2 ± 4.2 ^{c,f}	24.2 ± 5.7	16.9 ± 10.9
μmol/L	Copper	extern	12.7 ± 3.3	188.8 ± 167	48.8 ± 26.4
		1 h	9.9 ± 5.5	28.3 ± 11.4	426 ± 393
		24 h	24.8 ± 0.65	17.3 ± 10.3	24.7 ± 9.5
	Zinc	extern	38.4 ± 17.5	139.2 ± 94	398 ± 369
		1 h	70.5 ± 37.3	134.6 ± 38.8 ^e	37.8 ± 25.2
		24 h	260 ± 117	120.8 ± 31.1	459 ± 271

^a Macrophages infected with *M. smegmatis*, *M. avium*, or *M. tuberculosis* for 1 or 24 h were investigated. Bacteria that had not entered the macrophages after 1 h of infection were used as source of data for extracellular bacteria. Each data point represents the concentration of the different elements in the same phagosomes, because data for the different elements are acquired simultaneously for each measurement. Thus, the number of measurements (*n*) is the same for all elements: *M. smegmatis* extern, *n* = 2; *M. smegmatis* 1 h, *n* = 4; *M. smegmatis* 24 h, *n* = 3; *M. avium* extern, *n* = 5; *M. avium* 1 h, *n* = 6; *M. avium* 24 h, *n* = 3; *M. tuberculosis* extern, *n* = 2; *M. tuberculosis* 1 h, *n* = 7; *M. tuberculosis* 24 h, *n* = 6. The concentrations are expressed as counts per second per A, where no standards were available. The concentrations of elements with available standards were calculated assuming an average mycobacterial thickness of 1 μm and are expressed as millimoles per liter or micromoles per liter. Mean ± SEM are shown.

^b *p* < 0.05 vs external *M. tuberculosis* and *M. avium*.

^c *p* < 0.05 vs *M. smegmatis* 1 h.

^d *p* < 0.05 vs external *M. tuberculosis*, *M. tuberculosis* 24 h, and *M. avium* 1 h.

^e *p* < 0.05 vs *M. tuberculosis* 1 h.

^f *p* < 0.05 vs *M. avium* 24 h.

Table II. Concentration of latex beads^a

Element ($\mu\text{g}/\text{cm}^2$)	Absolute Concentration on Latex Bead	Concentration with Respect to Background		Ratio of Concentrations bg 2/bg 1 (%)
		bg 1 (green)	bg 2 (blue)	
Aluminum	1.7165	-1.6823	-1.1875	70.59
Silicon	1.5597	-1.1496	-1.0257	89.22
Phosphorus	0.5591	-0.5061	-0.3689	72.89
Sulfur	0.8853	-1.2099	-0.7095	58.64
Chlorine	7.0960	-10.6018	-6.2274	58.74
Argon	0.2244	-0.3438	-0.1986	57.76
Potassium	0.2468	-0.2687	-0.1956	72.80
Calcium	0.0250	-0.0511	-0.0299	58.53
Titanium	0.0034	-0.0206	0.0103	49.85
Chromium	0.0015	-0.0068	-0.0034	50.43
Manganese	0.0005	-0.0018	-0.0010	55.93
Iron	0.0116	-0.0107	-0.0111	103.55
Cobalt	0.0011	-0.0014	-0.0011	82.19
Nickel	0.0011	-0.0009	-0.0008	94.87
Copper	0.0014	-0.0009	-0.0007	74.49
Zinc	0.0165	-0.0151	-0.0120	79.41

^a Absolute concentration, as well as difference to surrounding cell material tissues (using both region of interest 1 (ROI1) and ROI2) are given. Difference concentrations are negative, because the latex beads contain no measurable quantities of any elements measured, and the surrounding cell material contains significant quantities of those. The first column shows absolute concentrations of all elements at the position of the latex bead defined by ROI (red). The concentration presumably reflects the material content of the cell layer above and below the latex bead. The second and third data column are latex concentrations normalized with the surrounding material. Because the elemental concentration in the surrounding material is significantly higher than on the latex bead, all values are negative. Choosing the "outer" background ROI (green) gives slightly larger differences than choosing the inner background ROI (blue), which is immediately adjacent to the latex bead. It could be speculated that the inner background ROI (blue) is located in the area where the phagosome is located. However, the spatial resolution is not sufficient to distinguish latex bead from phagosome from the cellular material in the vicinity of the vacuole with the latex bead.

concentration after 1 h of infection but failed to observe the increased concentration of iron observed in the H37Rv wild-type-containing vacuole (Table III). The iron concentration resembled more closely that measured in the *M. smegmatis* vacuole.

Comparison of the concentration of other elements between the H37Rv wild-type-containing vacuole and the H37Rv O1A mutant revealed a significantly increased zinc and a significantly decreased chlorine concentration in the mutant vacuoles 1 and 24 h after infection. The zinc concentration in extracellular O1A mutants was also higher than in the wild type, however, without being statistically significant ($p = 0.07$, data not shown). The calcium concentration was higher in the mutant vacuoles at the 1-h time point. A significant change in the concentrations of any element within the first 24 h of infection was not observed in the mutant vacuoles (Table IV).

Incorporation of iron by phagosomes

It is known that intracellular *M. avium* reside in vacuoles that lie within the transferrin recycling pathway of their host macrophage

(26), and mycobacteria synthesize siderophores and mycobactins capable of competing iron off transferrin (11). A recent study suggested that the internalized transferrin constitutes a source of iron that is associated with intracellular *M. tuberculosis*. However, it has not been formally shown that the iron is exploited and internalized by the bacterium (19). The distribution of ⁵⁹Fe can be determined through analysis of the traces appearing in the photographic emulsion layered over the sections examined under the electron microscope. Analysis of *M. avium*-infected cells following 16 h of continuous incubation with [⁵⁹Fe]transferrin revealed that the majority of internalized ⁵⁹Fe was associated with structures within the cytoplasm of the cell, as illustrated in Fig. 4A; although, even at this time point, many of the bacteria were positive for ⁵⁹Fe (Fig. 4B). When the data were corrected for the relative difference in surface area and expressed as the number of radioactive decays detected in a 10- μm^2 area of either cell cytoplasm, nuclei, or bacteria, it became clear that, even at 16 h, there was a disproportionate amount of label associated with the bacteria (Fig. 5). This enrichment of ⁵⁹Fe was even more marked at 48 h

Table III. Iron concentration in the mycobacterial phagosome^a

Treatment	Mycobacterial Species			
	<i>M. smegmatis</i>	<i>M. avium</i>	<i>M. tuberculosis</i>	<i>Mtb</i> H37Rv O1A
Extern	198 \pm 10	413 \pm 145	505 \pm 215	349 \pm 145
1 h	527 \pm 66.8 ^b	299 \pm 61.5	135 \pm 41.7	553 \pm 140 ^c
24 h	41.5 \pm 22.4 ^d	1167 \pm 474 ^e	2680 \pm 973 ^f	289 \pm 229 ^c

^a Data for macrophages infected for 1 or 24 h with *M. smegmatis*, *M. avium*, *M. tuberculosis*, or the siderophore knockout mutant of *M. tuberculosis*, *Mtb* H37Rv O1A, are shown. Values (mean \pm SEM) are expressed as micromoles per liter. For further reference and number of measurements (n) for the first three mycobacterial species, see Table I. For *Mtb* H37Rv O1A, the following numbers of phagosomes were mapped: extern, $n = 4$; 1 h, $n = 10$; 24 h, $n = 5$.

^b $p < 0.05$ vs *M. avium* 1 h and *M. tuberculosis* 1 h.

^c $p < 0.05$ vs *M. tuberculosis*.

^d $p < 0.05$ vs *M. smegmatis* 1 h.

^e $p < 0.05$ vs *M. avium* 1 h.

^f $p < 0.05$ vs *M. smegmatis* 24 h and *M. tuberculosis* 1 h.

Table IV. Intravacuolar concentrations of single elements on macrophages infected with *M. tuberculosis* H37Rv (*Mtb* wild type) and O1A mutant^a

Elements	1 h after Infection		24 h after Infection	
	<i>Mtb</i> wild type	O1A	<i>Mtb</i> wild type	O1A
Phosphorus ^b	7.0 ± 1.7	3.5 ± 0.995	7.1 ± 1.4	5.8 ± 1.8
Sulfur ^b	36.9 ± 5.5	7.6 ± 2.3	23.7 ± 3.9	15.2 ± 7.7
Chlorine ^b	404 ± 56	13.8 ± 2.2 ^c	197 ± 62	10.9 ± 1.5 ^c
Potassium ^d	19.5 ± 16.9	2.9 ± 0.8	51.0 ± 28.6	4.0 ± 1.4
Calcium ^d	1.8 ± 1.3	12.2 ± 2.4 ^c	7.1 ± 3.3	12.4 ± 2.4
Manganese ^d	14.7 ± 5.2	5.8 ± 2.8	16.9 ± 10.9	8.1 ± 2.6
Nickel ^b	0.15 ± 0.05	0.28 ± 0.09	0.07 ± 0.05	0.29 ± 0.08
Copper ^d	426 ± 393	59.6 ± 23.4	24.7 ± 9.5	12.9 ± 4.4
Zinc ^d	37.8 ± 25.2	2480 ± 674 ^c	459 ± 271	1345 ± 197 ^c

^a Macrophages were infected with *M. tuberculosis* or the siderophore knockout mutant of *M. tuberculosis*, *Mtb* H37Rv O1A, for 1 or 24 h. For further reference and number of measurements, see *Materials and Methods* and *Tables I and II*.

^b Concentrations are expressed as counts per second per A.

^c $p < 0.05$ compared with *Mtb* wild type.

^d Concentrations are expressed as micromoles per liter.

following a 32-h chase in the absence of additional labeled transferrin, and ⁵⁹Fe was observed with even greater frequency among the intracellular *M. avium*. These data indicate that *M. avium* acquires iron from transferrin and retains it at a concentration higher than that observed in the host macrophage cytosol.

Effect of macrophage activation with IFN- γ or TNF- α on the intravacuolar concentration of elements

Activation of the host macrophage by macrophage-activating cytokines has been shown previously to lead to increased acidification and maturation of *Mycobacterium*-containing vacuoles while the bacteria are still viable (27). To determine the effect of mac-

rophage activation on the concentration of elements, we used the following two procedures: 1) macrophages were stimulated with IFN- γ or TNF- α for 24 h and then infected with *M. avium* for 24 h; and 2) macrophages were infected with *M. avium* for 24 h and then stimulated with recombinant cytokines for an additional 24 h.

TNF- α treatment altered the concentration of elements in *M. avium* phagosomes compared with their concentrations in untreated macrophages. The phosphorus and sulfur concentrations decreased, and the zinc concentration increased if TNF- α was added to infected macrophages but did not change if TNF- α was added before infection. The decrease in the chlorine concentration when TNF- α was added after infection was not significant ($p = 0.07$). TNF- α treatment prevented

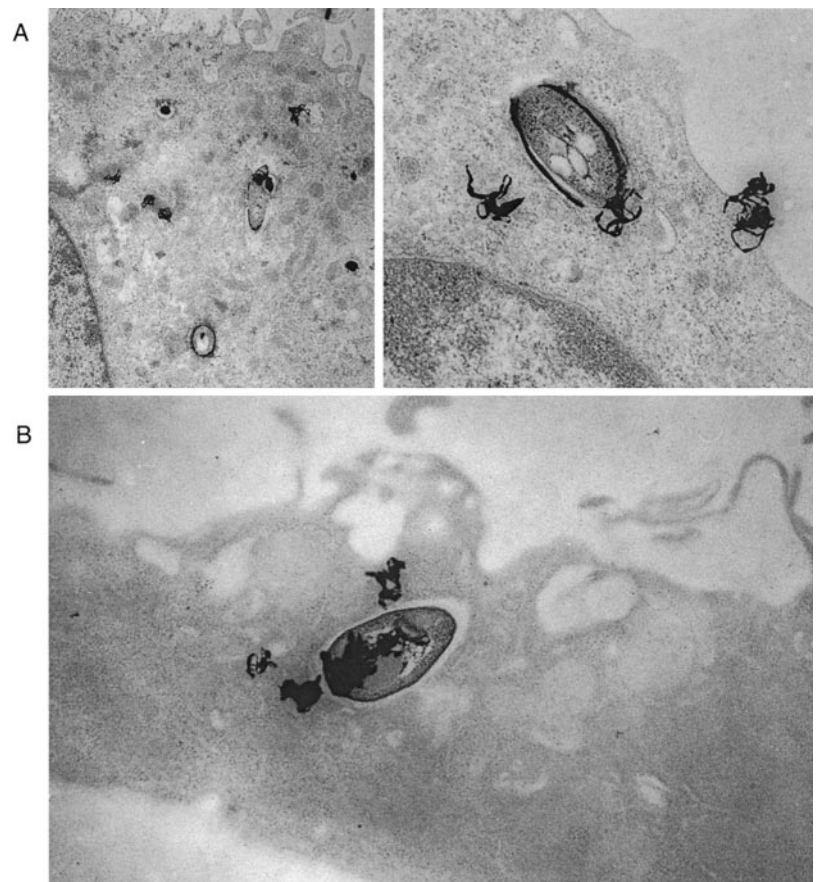


FIGURE 4. A, Electron microscopy of *M. avium*-infected mouse macrophages incubated with [⁵⁹Fe]transferrin. The majority of iron added to infected cells ended associated with cytoplasmic structures. B, *M. avium* vacuole showing significant incorporation of radioactive iron after a 32-h chase.

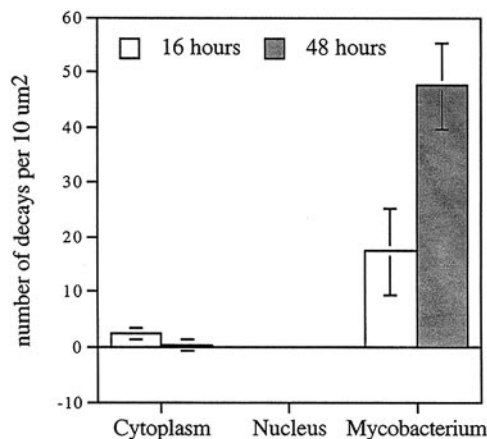


FIGURE 5. The distribution of ^{59}Fe -associated decays in macrophages infected with *M. avium* following incubation for 16 h with $10\ \mu\text{g/ml}$ [^{59}Fe]transferrin or at 48 h following a 32-h chase in the absence of [^{59}Fe]transferrin. The data are corrected for the differing surface area of the bacteria vs the cell and are displayed as the average number of events per $10\ \mu\text{m}^2$. The data indicate that the bacteria access and acquire iron from transferrin and that this iron is considerably more concentrated within the bacterium than in the cytosol of the host cell. Moreover, the bacterium appears to sequester and retain the iron relative to the host cell.

the increase of the iron concentration in *M. avium*-containing phagosome if added before infection and reversed the increase of the iron concentration seen in phagosome after 24 h of infection when added to *M. avium*-infected macrophages (Table V).

Exposure of macrophage monolayers to IFN- γ had different consequences on the concentration of elements in the phagosome when compared with untreated controls: phosphorus, sulfur, and chlorine concentrations were decreased, and zinc concentration was increased by IFN- γ treatment after infection but did not alter when IFN- γ was added before infection. The potassium concentration was higher, and the calcium concentrations were lower with IFN- γ treatment before infection when compared with vacuoles in which the cytokine was added to infected macrophages. This notably differs from the effect of TNF- α treatment after infection. The nickel concentration decreased, and the copper concentration increased with IFN- γ treatment regardless of time point of treatment. The increase that was observed of copper with IFN- γ treatment was significantly higher, when the cytokine was added after infection (Table VI).

Discussion

Despite an increasing number of studies indicating that pathogenic microorganisms such as *Salmonella*, *Shigella*, *Yersinia*, *Vibrio* (28), as well as *M. avium* (29), rely on environmental cues, including the concentrations of single elements in the environment, to regulate the expression of virulence genes and phenotype, little information is available concerning the concentration of these elements in the intracellular compartments in which these pathogens reside. Data in the current study were obtained for a range of elements in vacuoles containing pathogenic and nonpathogenic *Mycobacterium* spp.

Our data were obtained by measuring the concentration of each element in a number of different vacuoles. Among the observations made was that different vacuoles infected with the same number of bacteria of the same species demonstrated heterogeneity in the concentrations of certain elements. This heterogeneity is likely a product of several factors. First, not all the bacteria in the inocula are viable, or at the same metabolic level, as evidenced by the heterogeneity observed in extracellular bacteria in culture medium.

Second, the modulation of the phagosome by the bacteria is also heterogeneous within a range, as demonstrated by the measurements of individual vacuole pH published by Oh and Straubinger (30) but also noted by Clemens and Horwitz (18) for the acquisition of transferrin and for the lysosome-associated membrane glycoprotein CD63. As many as 40% of the *M. tuberculosis* phagosomes lack staining for transferrin, and half of these stained richly for CD63 (18). Nonetheless, despite the variation between vacuoles, the trends from mycobacterial species of varying pathogenicity are clear and reproducible.

Among our findings, most notable was the observation that although the concentration of iron in *M. smegmatis* phagosomes significantly decreased with time after bacterial ingestion by macrophages, the concentration of iron in both *M. avium* and *M. tuberculosis* vacuoles increased between 1 and 24 h following uptake. Considering the importance of iron for the survival of living organisms, this finding suggests that the pathogenic mycobacteria, in contrast to the nonpathogenic mycobacteria, possess mechanisms aimed at increasing the concentration of iron in the phagosome.

The bacteria's success in iron acquisition is demonstrated in our study using radioactive iron-loaded transferrin, which showed that extracellular iron is incorporated by infected macrophages and is delivered to *M. avium* vacuoles through the activity of the transferrin receptor. This observation confirms the findings from recently published studies (19) and the findings obtained by x-ray microscopy that indicate that vacuoles of virulent mycobacteria have the capacity to access and retain iron. In normal phagosome biogenesis, the phagosome shows transient access to the rapid recycling pathway and transferrin (26). The non-acidified phagosomes of *M. avium* or *M. tuberculosis* are arrested in their normal maturation, but remain fusion competent and fuse with vesicles of the early endosomal system. At pH 6.3, the pH of the sorting endosome and of the *M. avium*-containing vacuole (10), iron dissociates from the iron-saturated holotransferrin, enabling the apo-transferrin receptor complex to recycle to the plasmalemma. However, even in the absence of this release step, Horwitz and colleagues (11) have shown that the siderophores of *M. tuberculosis* have an affinity for iron high enough to compete the metal off transferrin at neutral pH. The iron acquisition molecules, siderophores, and mycobactins are thought to compete with the host's mechanisms to diminish the vacuolar iron concentration. A role for siderophore in iron acquisition was demonstrated in the recent work by De Voss et al. (16), who demonstrated that mycobactin-deficient *M. tuberculosis* were impaired for intracellular survival. Our data show that the absence of siderophores in this knockout mutant have a direct impact on the ability of the mycobacteria to acquire or retain intravacuolar iron, supporting the hypothesis that the vacuolar iron is available to mycobacteria, and siderophores are important to prevent the host from pumping iron out of the phagosome.

In macrophages that were activated with IFN- γ before the infection, the accumulation of iron after 1 day of infection was prevented in the phagosomes of the pathogenic mycobacteria. IFN- γ is known to down-regulate the expression of the transferrin receptor and to decrease the intracellular labile iron pool. It is also known that once macrophages have been activated with IFN- γ , they can acidify the *M. avium* vacuoles to pH ~ 5.2 and mature further down the endosomal continuum (27). This transition enhances the microbicidal capacity of the macrophage (31). However, the inability to induce a change in iron concentration in macrophages treated with IFN- γ after infection is likely a reflection of the reported energy that infected macrophages show to activating IFN- γ (32). It is interesting to note that the

Table V. Concentrations of single elements in *M. avium* vacuoles within macrophages treated with TNF- α before or after infection^a

Elements	<i>M. avium</i> 24 h	TNF- α + <i>M. avium</i>	<i>M. avium</i> + TNF- α
Phosphorus ^b	10.9 \pm 2.1	12.6 \pm 4.7	4.6 \pm 0.8 ^c
Sulfur ^b	35.9 \pm 9.5	23.5 \pm 5.5	5.7 \pm 1.5 ^{c,d}
Chlorine ^b	245 \pm 150	221 \pm 71.4	17 \pm 6.0
Potassium ^e	5.5 \pm 2.9	12.4 \pm 2.4	7.1 \pm 2.0
Calcium ^e	2.5 \pm 1.1	7.0 \pm 2.5	5.9 \pm 1.2
Manganese ^f	24.2 \pm 5.8	26.1 \pm 8.3	12.3 \pm 6.0
Iron ^f	1167 \pm 474	294 \pm 89.0 ^c	271 \pm 48.0 ^c
Nickel ^b	1.0 \pm 0.3	0.4 \pm 0.2	0.5 \pm 0.1
Cu ^f	17.3 \pm 10.3	61.3 \pm 24.6	82.3 \pm 20.3
Zn ^f	120.8 \pm 31.1	357 \pm 138	1826 \pm 737 ^d

^a Macrophages were treated with 100 U of TNF- α for 24 h before (TNF- α + *M. avium*) or after infection (*M. avium* + TNF- α). Results (mean \pm SEM) are based on the measures of 5–10 phagosomes in different macrophages in different preparations.

^b Concentrations are expressed as counts per second per A.

^c $p < 0.05$ compared with untreated *M. avium*-infected macrophages (*M. avium* 24 h).

^d $p < 0.05$ compared with TNF- α + *M. avium*.

^e Concentrations are expressed as millimoles per liter.

^f Concentrations are expressed as micromoles per liter.

intravacuolar concentrations of single elements in macrophages activated with IFN- γ or TNF- α show variation between elements such as chlorine, calcium, nickel, and copper. Also, the fact that TNF- α in contrast to IFN- γ was capable of reversing the accumulation of iron in the mycobacterial phagosome after infection suggests that the mechanisms or degrees of macrophage activation by both cytokines are not comparable.

Little is known about the concentration or regulation of other elements in the phagosomes of intracellular bacteria, although these are crucial for many cell functions. Among other differences that were observed for the concentration of several elements in the phagosome of different mycobacterial species and during macrophage activation, the most notable was the increased zinc concentrations in the siderophore knockout *M. tuberculosis* strain. It may be that, in this mutant, Zn²⁺ is used as a substitute for metabolic purposes in storage proteins and enzymes for the unavailable Fe²⁺, as suggested by the higher zinc concentrations in extracellular mutant bacteria. However, the fact that a similar increase in the zinc concentration was observed in the presence of TNF- α or IFN- γ in infected macrophages implies specific regulatory mechanisms for the delivery of this element to the mycobacterial phagosome. In

this respect, the observation that a Cu,Zn-SOD contributes to the resistance of *M. tuberculosis* against oxidative burst products generated by activated macrophages is intriguing (14).

Possible candidates for this sequestering of iron and/or other divalent cations from the endosomal system into the cell cytosol are members of the divalent cation transport family of proteins, natural resistance-associated macrophage protein 1 (NRAMP1; which now is classified as the solute carrier family 11 member 1, *Slc11a1*) and NRAMP2 (DMT1), which are expressed in macrophages at different stages of the endosomal continuum (33, 34). Colocalization of mycobacterial phagosomes has only been shown with the NRAMP1 protein in some *M. avium*-containing phagosomes (34), but whether NRAMP1 functions as an efflux pump or as an influx pump is an ongoing debate (35–37). NRAMP1 recruitment may increase the fusogenic properties of the mycobacterial phagosome (35) and affects intracellular survival of *M. avium* in bone marrow-derived mouse macrophages after an initial lag period of 2–4 days (38), possibly by the modulation of the phagosomal pH (39). In our study, *NRAMP1*^s mice were used, and the question whether and how the presence of a functional NRAMP1 protein affects the phagosomal concentration of single elements was not addressed.

Table VI. Concentration of single elements in *M. avium* vacuoles within macrophages treated with IFN- γ before or after infection^a

Elements	<i>M. avium</i> 24 h	IFN- γ + <i>M. avium</i>	<i>M. avium</i> + IFN- γ
Phosphorus ^b	10.9 \pm 2.1	12.4 \pm 0.9	4.5 \pm 0.8 ^{c,d}
Sulfur ^b	35.9 \pm 9.5	39.8 \pm 7.3	3.2 \pm 0.3 ^{c,d}
Chlorine ^b	245 \pm 150	443 \pm 82.7	5.7 \pm 0.9 ^{c,d}
Potassium ^e	5.5 \pm 2.9	20.4 \pm 5.8	2.1 \pm 0.4 ^d
Calcium ^e	2.5 \pm 1.1	3.0 \pm 0.6	5.7 \pm 1.0 ^d
Manganese ^f	24.2 \pm 5.8	13.1 \pm 4.9	20.4 \pm 9.2
Iron ^f	1167 \pm 474	197 \pm 55.2 ^c	742 \pm 266
Nickel ^b	1.0 \pm 0.3	0.067 \pm 0.038 ^c	0.13 \pm 0.04 ^c
Copper ^f	17.3 \pm 10.3	81.8 \pm 14.1 ^e	177 \pm 40.5 ^{c,d}
Zinc ^f	120.8 \pm 31.1	83.4 \pm 52.4	505 \pm 76.3 ^{c,d}

^a Recombinant murine IFN- γ was added either 24 h before (IFN- γ + *M. avium*) or after infection (*M. avium* + IFN- γ). Results represent average \pm SEM of 5–10 vacuoles on different macrophages and different preparations.

^b Concentrations are expressed as counts per second per A.

^c $p < 0.05$ compared with untreated *M. avium*-infected macrophages (*M. avium* 24 h)

^d $p < 0.05$ compared with IFN- γ + *M. avium*

^e Concentrations are expressed as millimoles per liter.

^f Concentrations are expressed as micromoles per liter.

Localization of NRAMP2 to early endosomes and its colocalization to the transferrin receptor in the mouse monocyte-macrophage cell line RAW 264.7 (33) implies that the NRAMP2 transporter may be present in the mycobacterial phagosome at earlier stages than NRAMP1. Concordantly, infection of mice peritoneal macrophages with *M. avium* has been shown to up-regulate the expression of *Nramp2*-mRNA several hours before the *Nramp1*-mRNA expression. Simultaneously, the synthesis and expression of transferrin receptor RNA was decreased (40). It remains to be seen whether NRAMP1 or NRAMP2 function as Fe^{2+} , Mn^{2+} , or Zn^{2+} transporter (41) or even as a Cu^{2+} or Ni^{2+} transporter in the mycobacterial phagosome and whether these are involved in the changes in the concentration of respective cations in phagosomes of virulent and avirulent mycobacteria, as observed in our study.

In conclusion, this study provides the first exact measurements of the intraphagosomal concentrations of single elements, a notable gap in our knowledge of the luminal content of the endosomal/lysosomal system that has a major impact on the health and well-being of intracellular pathogens. Most notably, our results suggest that pathogenic mycobacteria but not the avirulent *M. smegmatis* accumulate iron in the phagosome at least in part through the activity of the transferrin receptor and that the siderophore production is necessary to retain the iron in the mycobacterial phagosome. In context with the observation that the siderophore-deficient mutant of *M. tuberculosis* is markedly attenuated for intramacrophage survival (16), this study highlights the importance of the iron concentration for the intracellular survival of pathogenic mycobacteria.

Acknowledgments

We thank Denny Weber for preparation of the manuscript.

References

- Mekalanos, J. J. 1992. Environmental signals controlling expression of virulence determinants in bacteria. *J. Bacteriol.* 174:1.
- Litwin, C. M., and S. B. Calderwood. 1993. Role of iron in regulation of virulence genes. *Clin. Microbiol. Rev.* 6:137.
- Miller, J. F., J. J. Mekalanos, and S. Falkow. 1989. Coordinate regulation and sensory transduction in the control of bacterial virulence. *Science* 243:916.
- Cornelis, G. R., A. Boland, A. P. Boyd, C. Geuijen, M. Iriarte, C. Neyt, M. P. Sory, and I. Stainier. 1998. The virulence plasmid of *Yersinia*, an antihist genome. *Microbiol. Mol. Biol. Rev.* 62:1315.
- Garcia Vescovi, E., F. C. Soncini, and E. A. Groisman. 1996. Mg^{2+} as an extracellular signal: environmental regulation of *Salmonella* virulence. *Cell* 84:165.
- Garcia-del Portillo, F., J. W. Foster, M. E. Maguire, and B. B. Finlay. 1992. Characterization of the micro-environment of *Salmonella typhimurium*-containing vacuoles within MDCK epithelial cells. *Mol. Microbiol.* 6:3289.
- Bloom, B. R. 1994. *Tuberculosis: Pathogenesis, Protection and Control*. Am. Soc. Microbiol., Washington, DC.
- Inderlied, C. B., C. A. Kemper, and L. E. Bermudez. 1993. The *Mycobacterium avium* complex. *Clin. Microbiol. Rev.* 6:266.
- Crowle, A. J., R. Dahl, E. Ross, and M. H. May. 1991. Evidence that vesicles containing living, virulent *Mycobacterium tuberculosis* or *Mycobacterium avium* in cultured human macrophages are not acidic. *Infect. Immun.* 59:1823.
- Sturgill-Koszycki, S., P. H. Schlesinger, P. Chakraborty, P. L. Haddix, H. L. Collins, A. K. Fok, R. D. Allen, S. L. Gluck, J. Heuser, and D. G. Russell. 1994. Lack of acidification in *Mycobacterium* phagosomes produced by exclusion of the vesicular proton-ATPase. *Science* 263:678.
- Gobin, J., and M. A. Horwitz. 1996. Exochelins of *Mycobacterium tuberculosis* remove iron from human iron-binding proteins and donate iron to mycobactins in the *M. tuberculosis* cell wall. *J. Exp. Med.* 183:1527.
- Gangaidzo, I. T., V. M. Moyo, E. Mvundura, G. Aggrey, N. L. Murphree, H. Khumalo, T. Saungweme, I. Kasvosve, Z. A. Gomo, T. Rouault, et al. 2001. Association of pulmonary tuberculosis with increased dietary iron. *J. Infect. Dis.* 184:936.
- Schaible, U. E., H. L. Collins, F. Priem, and S. H. Kaufmann. 2002. Correction of the iron overload defect in β_2 -microglobulin knockout mice by lactoferrin abolishes their increased susceptibility to tuberculosis. *J. Exp. Med.* 196:1507.
- Bunting, K., J. B. Cooper, M. O. Badasso, I. J. Tickle, M. Newton, S. P. Wood, Y. Zhang, and D. Young. 1998. Engineering a change in metal-ion specificity of the iron-dependent superoxide dismutase from *Mycobacterium tuberculosis*: X-ray structure analysis of site-directed mutants. *Eur. J. Biochem.* 251:795.
- Escuyer, V., N. Haddad, C. Frehel, and P. Berche. 1996. Molecular characterization of a surface-exposed superoxide dismutase of *Mycobacterium avium*. *Microb. Pathog.* 20:41.
- De Voss, J. J., K. Rutter, B. G. Schroeder, H. Su, Y. Zhu, and C. E. Barry 3rd. 2000. The salicylate-derived mycobactin siderophores of *Mycobacterium tuberculosis* are essential for growth in macrophages. *Proc. Natl. Acad. Sci. USA* 97:1252.
- Wong, D. K., B. Y. Lee, M. A. Horwitz, and B. W. Gibson. 1999. Identification of fur, aconitase, and other proteins expressed by *Mycobacterium tuberculosis* under conditions of low and high concentrations of iron by combined two-dimensional gel electrophoresis and mass spectrometry. *Infect. Immun.* 67:327.
- Clemens, D. L., and M. A. Horwitz. 1996. The *Mycobacterium tuberculosis* phagosome interacts with early endosomes and is accessible to exogenously administered transferrin. *J. Exp. Med.* 184:1349.
- Olakanmi, O., L. S. Schlesinger, A. Ahmed, and B. E. Britigan. 2002. Intraphagosomal *Mycobacterium tuberculosis* acquires iron from both extracellular transferrin and intracellular iron pools: impact of interferon- γ and hemochromatosis. *J. Biol. Chem.* 277:49727.
- Rodriguez, G. M., and I. Smith. 2003. Mechanisms of iron regulation in mycobacteria: role in physiology and virulence. *Mol. Microbiol.* 47:1485.
- Bermudez, L. E., A. Parker, and J. R. Goodman. 1997. Growth within macrophages increases the efficiency of *Mycobacterium avium* in invading other macrophages by a complement receptor-independent pathway. *Infect. Immun.* 65:1916.
- Azouaou, N., M. Petrofsky, L. S. Young, and L. E. Bermudez. 1997. *Mycobacterium avium* infection in mice is associated with time-related expression of Th1 and Th2 CD4⁺ T-lymphocyte response. *Immunology* 91:414.
- Cai, Z., B. Lai, W. Yun, P. Ilniski, D. Legnini, J. Maser, and W. Rodrigues. 1999. Proceedings of the VI International Conference. In *American Institute of Physics*, Vol. 507. W. Meyer-Ilse, T. Warwick, and D. Attwood, eds. X-ray Microscopy, Berkeley, CA, p. 472.
- Dyer, D. W., W. McKenna, J. P. Woods, and P. F. Sparling. 1987. Isolation by streptonigrin enrichment and characterization of a transferrin-specific iron uptake mutant of *Neisseria meningitidis*. *Microb. Pathog.* 3:351.
- Sullivan, D. J., Jr., I. Y. Gluzman, D. G. Russell, and D. E. Goldberg. 1996. On the molecular mechanism of chloroquine's antimalarial action. *Proc. Natl. Acad. Sci. USA* 93:11865.
- Sturgill-Koszycki, S., U. E. Schaible, and D. G. Russell. 1996. *Mycobacterium*-containing phagosomes are accessible to early endosomes and reflect a transitional state in normal phagosome biogenesis. *EMBO (Eur. Mol. Biol. Organ.) J.* 15:6960.
- Schaible, U. E., S. Sturgill-Koszycki, P. H. Schlesinger, and D. G. Russell. 1998. Cytokine activation leads to acidification and increases maturation of *Mycobacterium avium*-containing phagosomes in murine macrophages. *J. Immunol.* 160:1290.
- Finlay, B. B., and S. Falkow. 1997. Common themes in microbial pathogenicity revisited. *Microbiol. Mol. Biol. Rev.* 61:136.
- Bermudez, L. E., M. Petrofsky, and J. Goodman. 1997. Exposure to low oxygen tension and increased osmolarity enhance the ability of *Mycobacterium avium* to enter intestinal epithelial (HT-29) cells. *Infect. Immun.* 65:3768.
- Oh, Y. K., and R. M. Straubinger. 1996. Intracellular fate of *Mycobacterium avium*: use of dual-label spectrofluorometry to investigate the influence of bacterial viability and opsonization on phagosomal pH and phagosome-lysosome interaction. *Infect. Immun.* 64:319.
- Via, L. E., D. Deretic, R. J. Ulmer, N. S. Hibler, L. A. Huber, and V. Deretic. 1997. Arrest of mycobacterial phagosome maturation is caused by a block in vesicle fusion between stages controlled by rab5 and rab7. *J. Biol. Chem.* 272:13326.
- Ting, L. M., A. C. Kim, A. Cattamanchi, and J. D. Ernst. 1999. *Mycobacterium tuberculosis* inhibits IFN- γ transcriptional responses without inhibiting activation of STAT1. *J. Immunol.* 163:3898.
- Gruenheid, S., F. Canonne-Hergaux, S. Gauthier, D. J. Hackam, S. Grinstein, and P. Gros. 1999. The iron transport protein NRAMP2 is an integral membrane glycoprotein that colocalizes with transferrin in recycling endosomes. *J. Exp. Med.* 189:831.
- Searle, S., N. A. Bright, T. I. Roach, P. G. Atkinson, C. H. Barton, R. H. Meloan, and J. M. Blackwell. 1998. Localisation of Nramp1 in macrophages: modulation with activation and infection. *J. Cell Sci.* 111:2855.
- Forbes, J. R., and P. Gros. 2001. Divalent-metal transport by NRAMP proteins at the interface of host-pathogen interactions. *Trends Microbiol.* 9:397.
- Gomes, M. S., and R. Appelberg. 2002. NRAMP1- or cytokine-induced bacteriostasis of *Mycobacterium avium* by mouse macrophages is independent of the respiratory burst. *Microbiology* 148:3155.
- Kuhn, D. E., W. P. Lafuse, and B. S. Zwillig. 2001. Iron transport into *Mycobacterium avium*-containing phagosomes from an Nramp1(Gly169)-transfected RAW264.7 macrophage cell line. *J. Leukocyte Biol.* 69:43.
- Frehel, C., F. Canonne-Hergaux, P. Gros, and C. De Chastellier. 2002. Effect of Nramp1 on bacterial replication and on maturation of *Mycobacterium avium*-containing phagosomes in bone marrow-derived mouse macrophages. *Cell. Microbiol.* 4:541.
- Hackam, D. J., O. D. Rotstein, W. Zhang, S. Gruenheid, P. Gros, and S. Grinstein. 1998. Host resistance to intracellular infection: mutation of natural resistance-associated macrophage protein 1 (Nramp1) impairs phagosomal acidification. *J. Exp. Med.* 188:351.
- Zhong, W., W. P. Lafuse, and B. S. Zwillig. 2001. Infection with *Mycobacterium avium* differentially regulates the expression of iron transport protein mRNA in murine peritoneal macrophages. *Infect. Immun.* 69:6618.
- Blackwell, J. M., S. Searle, T. Goswami, and E. N. Miller. 2000. Understanding the multiple functions of Nramp1. *Microbes Infect.* 2:317.